CFD modeling of the building integrated with a novel design of a one-sided wind-catcher with water spray

Focus on thermal comfort

Foroozesh, Jamal; Hosseini, S. H.; Ahmadian Hosseini, A. J.; Parvaz, F.; Elsayed, K.; Uygur Babaoğlu, Nihan; Hooman, K.; Ahmadi, G.

DOI
10.1016/j.seta.2022.102736

Publication date
2022

Document Version
Final published version

Published in
Sustainable Energy Technologies and Assessments

Sustainable Energy Technologies and Assessments 53 (2022) 102736

Contents lists available at ScienceDirect

Sustainable Energy Technologies and Assessments

journal homepage: www.elsevier.com/locate/seta

CFD modeling of the building integrated with a novel design of a one-sided wind-catcher with water spray: Focus on thermal comfort

Jamal Foroozesh [a], S.H. Hosseini [b,*], A.J. Ahmadian Hosseini [c], F. Parvaz [d], K. Elsayed [e], Nihan Uygur Babaoğlu [f], K. Hooman [g], G. Ahmadi [h]

[a] Department of Metallurgy and Materials Science, Faculty of Engineering, Shahid Bahonar University of Kerman, Kerman, Iran
[b] Department of Chemical Engineering, Faculty of Engineering, Ilam University, Ilam 69315–516, Iran
[c] Department of Mechanical Engineering, Ferdowsi University of Mashhad, Mashhad, Iran
[d] Department of Mechanical Engineering, Semnan University, P.O. Box 35131-191, Semnan, Iran
[e] Mechanical Power Engineering Department, Faculty of Engineering at El-Mattaria, Helwan University, Masaken El-Helmia P.O., Cairo 11718, Egypt
[f] Department of Environmental Engineering, Kahramanmaras Sutcu Imam University, Kahramanmaras, Turkey
[g] Dept. of Process and Energy, Delft University of Technology, 2628 CB Delft, Netherlands
[h] Department of Mechanical and Aerospace Engineering, Clarkson University, Potsdam, NY 13699-5725, USA

ARTICLE INFO

Keywords:
Natural ventilation
Evaporative cooling
Novel wind-catcher
CFD
Thermal comfort

ABSTRACT

The rising energy demand for buildings has enhanced public awareness of sustainable energy sources and technologies. In particular, natural ventilation systems such as wind-catchers have attracted considerable new attention. A new wind-catcher design with single-stage direct-air evaporative cooling was proposed for indoor air conditioning. An Eulerian-Lagrangian approach employing the Realizable $k-\varepsilon$ model was utilized to conduct the CFD simulations. Furthermore, the effects of inclining the bottom surface of the wind-catcher and installing a baffle across the flow path on the air temperature drop, water mass fraction, and air velocity distribution were studied. The inclined bottom surface led to more flow uniformity in the room compared to the conventional geometry. The baffled wind-catcher with $\beta = 0$, 30, 45, and 60° and unbaffled wind-catcher showed different flow patterns and thermal comforts. A methodology for evaluating the thermal comfort performance of evaporative cooling systems integrated into natural or passive cooling devices was also proposed based on the generated CFD results. The baffled wind-catcher with $\beta = 60°$ combined with an evaporative cooling system significantly reduced the air temperature inside the building up to 17.4 °C and improved the occupants' thermal comfort. The most suitable design for thermal comfort was also determined.

Introduction

Significant growth in global demand for energy and increasing world population and air pollution has reached an "alarming level." According to the Paris agreement, governments agreed to cut emissions so that the global temperature increase stays within 2 °C. The 2008 UK Climate Change Act plans to reduce carbon emissions by 80 % by 2050 [1]. Thus, moving toward renewable energy away from fossil fuels has become a major priority [2]. Buildings are major energy consumers worldwide, responsible for about 45 % of global carbon emissions [3]. In addition, the energy consumption of cooling ventilation and providing indoor comfort increases in hot and dry climates. The buildings' ventilation and cooling systems consume more than half of summer's energy demand [4]. Overall, thermal insulation and natural ventilation systems can save 90.7 and 20.2 % of energy demand, respectively, in hot arid climates [5]. Despite the importance of reducing energy usage for ventilation systems, indoor air quality and resident thermal comfort should not be undermined [6,7].

Thermal comfort plays a critical role in the design and operation of indoor environments [8]. Passive cooling or natural ventilation has gained popularity in providing thermal comfort without increasing energy consumption [9–11]. The natural ventilation techniques, such as wind-catchers, which can enhance the rate of fresh airflow and reduce energy consumption, have attracted considerable attention [12]. A wind-catcher can be described as an architectural element located at a high elevation (e.g., rooftops) [13] that supplies fresh air to the indoor

* Corresponding author.
E-mail address: s.h.hosseini@ilam.ac.ir (S.H. Hosseini).

https://doi.org/10.1016/j.seta.2022.102736
Received 25 April 2022; Received in revised form 28 August 2022; Accepted 1 September 2022
Available online 12 September 2022

environment and discharges stale air as an exhaust stream [14]. As an architectural solution for hot and dry climates, such as Yazd City in Iran, known as the wind-catcher city, these towers have long been used to provide thermal comfort and boost ventilation levels [15,16]. Different designs of wind-catcher were developed to meet various requirements of different regions. In middle east countries, wind-catchers have been developed and utilized for several centuries [17,18].

Over the past 40 years, new wind-catchers have been developed and constructed in the UK. Increased energy costs, passive cooling awareness, and demand for healthy indoor environments led to the implementation of wind-catchers in modern buildings [19]. Wind-catchers provide ventilation and airflow movement inside buildings using air buoyancy or wind flow [20]. The wind-catcher ventilation relies on the pressure differential between the inlet and outlet to draw fresh air into a building and exhaust old air [21]. Hence, the position of the wind-catcher and the pressure loss between the inlet and outlet are key factors for maximizing ventilation [16].

Depending on the number of openings, wind-catchers are one, two, four, six, and eight-sided. In addition, according to Montazeri [14], a rectangular wind-catcher typically provides better ventilation than a circular one. Therefore, a one-sided wind-catcher with a rectangular base is used in the present study. The evaporative cooling method is an efficient and historically recognized technique to supply cooling and comfort in buildings in hot climates [22]. The water evaporation absorbs heat from the incoming airflow and reduces the air temperature with less energy consumption than refrigeration systems. In addition, increasing the air humidity improves the occupants' thermal comfort in dry climates [23]. Integrating underground water canals with wind-catchers was a traditional approach to cool and humidify the indoor environment to enhance comfort [23,24].

A significant amount of research on wind-catchers was focused on their ventilation and cooling performance [13,25,26]. Ventilation studies focused on the physical characteristics of the wind-catcher, such as the inlet openings, louvers, dampers, shape, height, and positioning to maximize the airflow [27–31]. Similarly, studies on the wind-catcher thermal performance were concerned with climatic analysis [2], integration of cooling devices such as evaporative cooling [32,33] and heat pipes [18], as well as heat recovery units [20]. Some recent studies were concerned with the indoor environments that are ventilated by the wind-catcher by assessing parameters such as the CO_2 concentration, indoor air temperature, and relative humidity [26,34]. However, only a few studies [16,35–37] addressed the indoor thermal comfort of buildings integrated with wind-catchers.

Earlier studies

Several authors reported using evaporative cooling as a natural ventilation approach in buildings. Hughes et al. [26] compared various cooling methods integrated with the wind-catchers to improve their thermal efficiency. Their results indicated that integrating the wetted column reduces air temperature by 12–15 °C. Bahadori et al. [38] examined two wind-catchers with evaporative cooling in Yazd, Iran. Wetted curtains were installed in the first wind-catcher duct while cooling pads were used at the inlet of the second one. It was found that the wetted curtains improved the wind-catcher thermal performance for high wind speeds, whereas cooling pads enhanced the performance at low wind speeds. Saffari and Hosseinnia [22] utilized an Eulerian-Lagrangian CFD model to study the influence of the height of wetted surfaces on the cooling efficiency of the Bahadori et al. [38] wind-catcher. They showed good agreement between the numerical results and the Bahadori et al. analytical solutions [38]. Their results indicated that 10 m high wetted curtains cooled the air by 12 °C.

Ahmadikia et al. [33] simulated the efficiency of a vernacular wind-catcher joined with two water ponds. The evaporative cooling system was more effective at lower wind speeds. In addition, adding water spray increased relative humidity by 5 % and lowered incoming air temperature by 4 °C. Kalantar [32] used numerical modeling and experimental studies to investigate a one-sided wind-catcher in Yazd, Iran. It was shown that water spray optimization reduced air temperature by up to 15 °C. In addition, the integrated system could generate up to 100 kW of cooling, sufficient for a 700 m^2 building in that hot and dry climate, using 0.025 kg/s of water mass flow. Bouchahm et al. [36] assessed the thermal performance and ventilation rate of a one-sided wind-catcher. The wind-catcher had clay conduits and a water pool for heat and mass transfer. Their results showed that a wind-catcher with wetted interior surfaces and a water pool could cool the room air temperature by 17.6 °C.

Jafari and Kalantar [39] studied the evaporative cooling rate of a multi-story building with three solar chimneys and a water spray at the entrance region of a wind-catcher in a hot/dry climate using a CFD model. Their model showed that the building air temperature could be reduced by 6–12 °C. Rabani [40] studied a novel passive solar cooling system using CFD. The model consisted of a solar chimney with tilted absorbers and a wet underground channel. It was found that the solar chimney could provide natural air ventilation in the space during the day without causing temperature stratification. Furthermore, employing a water spraying system to room air reduced the indoor temperature by 7–13 °C. It should be noted that the variation of the relative humidity due to the evaporative of water droplets has not been included in most earlier CFD-based indoor thermal comfort studies; instead, the relative humidity was estimated from meteorological data for a particular region.

Sadeghi et al. [35] explored the efficiency of a wind-catcher and thermal comfort for a typical medium-size apartment building in Sydney, Australia. They performed a wind tunnel study of the four-story apartment building and measured the surface pressure distribution. They also evaluated the thermal comfort provided by wind-catchers using the Standard Effective Temperature (SET) index recommended by ASHRAE [41] for evaluating the comfort condition for air speeds above 0.2 m/s in indoor spaces. Reyes et al. [37] numerically investigated the feasibility of using wind-catchers in arid and semi-arid climates in Northern Mexico. They analyzed the performance of five wind-catchers with different geometrical configurations and recommended the most effective one for building airflow and thermal comfort analysis.

Hosseini et al. [16] reported a CFD model for a building integrated with a two-sided wind-catcher in Yazd, Iran. They studied the effect of different wind-catcher geometry on the airflow patterns through a building. In parallel with the CFD model, the tool developed by the Center for Built Environment (CBE) [42] was used to optimize the wind-catcher design. Using a set of 3-D CFD simulations, Goudarzi et al. [27] studied the influence of size and elevation of outlet openings on airflow behavior and occupants' thermal comfort in a building with a two-sided wind-catcher. Sheikhshahrokhdehkordi et al. [43] developed a validated CFD model and studied the airflow rate and velocity in a two-sided wind-catcher under different conditions. Nejat et al. [44] numerically investigated the indoor air quality (IAQ) and adaptive thermal comfort in a room integrated with a two-sided wind-catcher. They considered a wind-catcher with an upper wing wall on top of an isolated building. Their simulations were done for the upper wing wall lengths of 10 cm to 50 cm and various wind speeds. Xu et al. [45] used a CFD technique to simulate the natural ventilation of a complex building and calculated the predicted mean vote (PMV) index for thermal comfort.

The present literature review shows that wind-catchers with evaporative cooling can significantly reduce the supply air temperature. However, the impact of wind-catchers on the occupant's thermal comfort when water spray is used for evaporative cooling has not been fully explored. Therefore, this study simulated the airflow and thermal conditions in a three-dimensional building, including a novel one-sided wind-catcher and main living space. In addition, the thermal comfort-based tool of CBE was used to obtain the optimal wind-catcher design. For this purpose, a set of simulations were performed by the Eulerian-Lagrangian computational approach, which included water spray

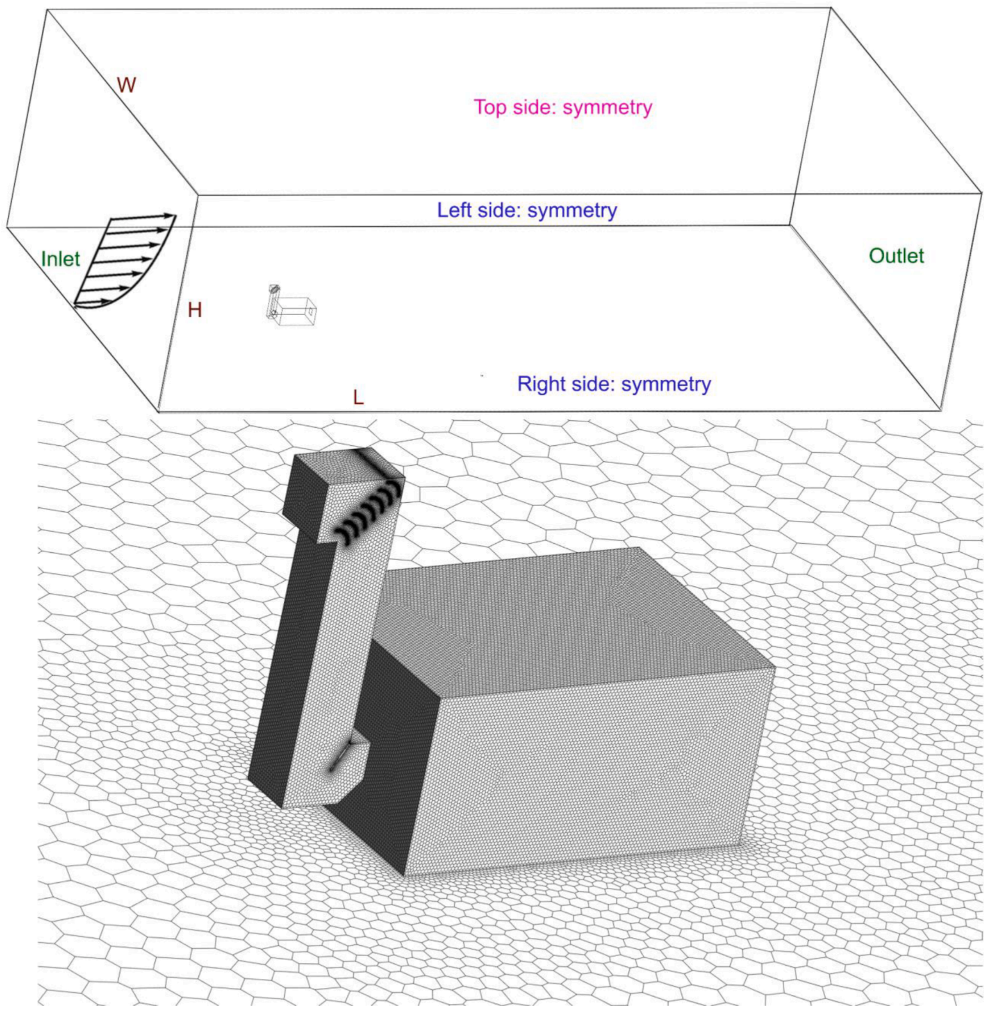

Fig. 1. The geometry of the simulated one-sided wind-catcher with and applied boundary conditions.

evaporation effects implemented in the wind-catcher tower. This study also addressed the occupant thermal comfort in the room connected with the novel wind-catcher.

Method

CFD model

In this study, the ANSYS-Fluent 21 CFD code was utilized to model the outdoor airflow into the wind-catcher and the building. The airflow simulation was performed using a three-dimensional computational model under steady-state conditions, including heat and moisture transport. The computational model uses the second-order upwind schemes and the SIMPLE velocity–pressure coupling algorithm. The Reynolds averaged Navier Stokes (RANS) equation was employed for these simulations. In addition, the Realizable $k-\varepsilon$ model that was shown to be accurate for indoor turbulent airflow simulation is used in the analysis [29,46]. The Lagrange approach is used for analyzing the droplet motions. The droplet-air interactions were modeled using the two-way coupling approach. The ANSYS-Fluent's hollow-cone spray model was used to inject water droplets with diameter of 50 μm into the system via a 4 mm diameter nozzle in the tower. The governing transport equations for steady incompressible turbulent airflow with heat and mass transfer are presented in the supplementary file.

Computational geometry

Fig. 1 shows a one-sided wind-catcher integrated with a building in a computational domain [47]. In addition to the building geometry, the polyhedral meshes generated by ANSYS-Fluent are shown in this figure [48].

The computational space was divided into three regions: the outdoor environment, the wind-catcher, and the room. The approach of integrating the wind-catcher with a room in the computational domain was used earlier [27,28,31]. The dimensions of the computational domain were W = 64 m, H = 36 m, and L = 127.75 m. As seen in the figure, the symmetry boundary conditions are used on the computational domain's right, left, and top sides since the building size is small. The wind velocity profile U (m/s), turbulent kinetic energy k (m^2/s^2), and turbulence dissipation rate ε (m^2/s^3) are imposed at the domain's inlet as [28]:

$$U(z) = \frac{u^*}{\kappa} ln\left(\frac{z + z_0}{z_0}\right) \quad (1)$$

$$k(z) = 3.3u^{*2} \quad (2)$$

$$\varepsilon(z) = \frac{u^{*3}}{\kappa(z + z_0)} \quad (3)$$

where the reference wind speed at z = 10 m is 3 m/s ($u^* = 0.2168$ m/s), $\kappa = 0.42$, and $z_0 = 0.03$ m.

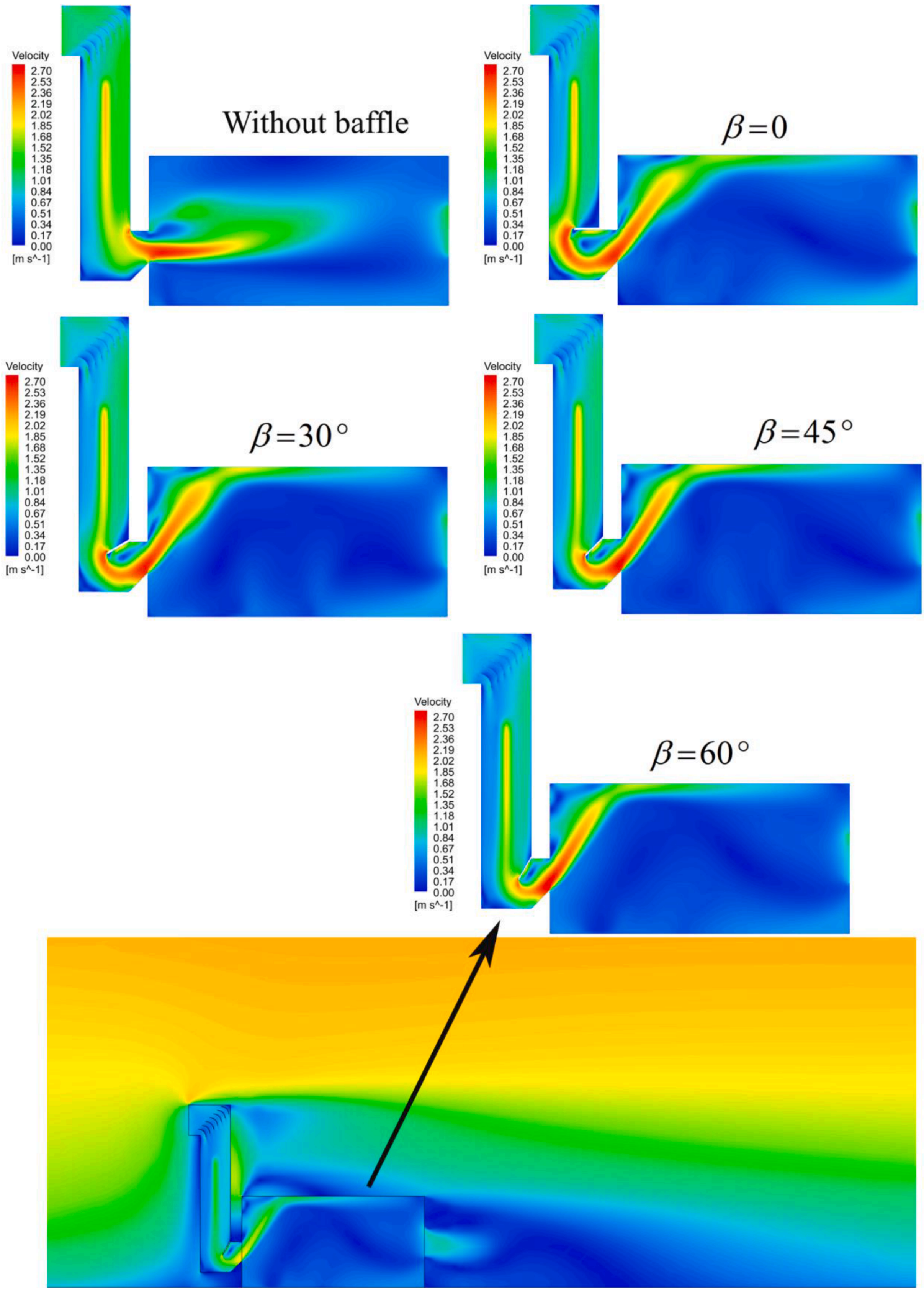

Fig. 2. The airflow velocity contours on the room mid-section for different wind-catcher baffle angles.

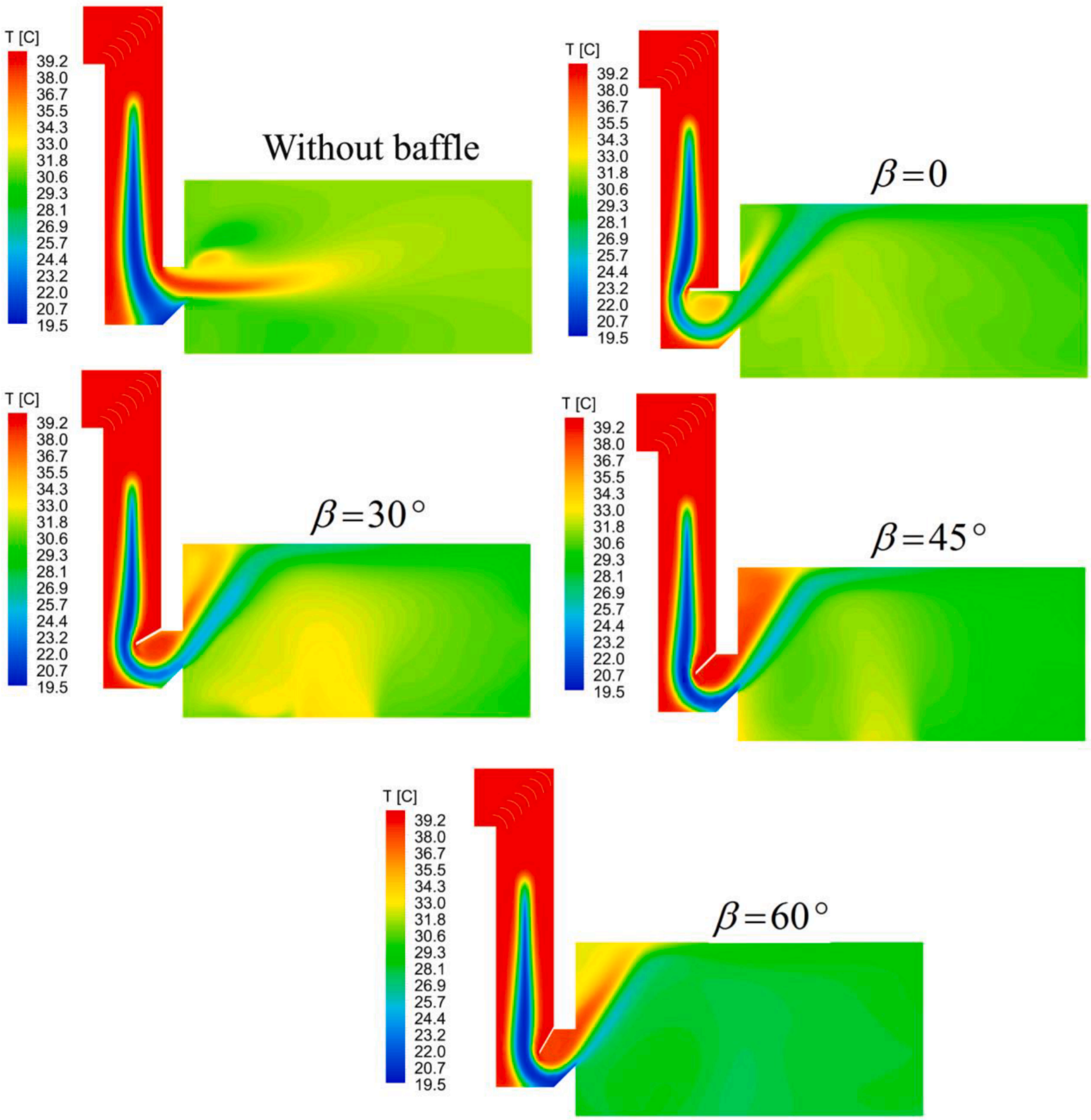

Fig. 3. Air temperature contours on the building mid-section for different wind-catcher baffle angles.

The no-slip condition is used on the ground, and the atmospheric outlet pressure is employed at the outlet region. An inlet temperature of 39.2 °C and relative humidity of 13.2 %, which represents the typical climatic condition in hot and dry areas, are used in all simulations. As recommended in the previous works [39,49], the spray water flow rates of 0.004 and 0.006 kg/s are injected into the tower for the subsequent simulations using a hollow-cone nozzle configuration used earlier in [46]. In addition, the uniform spray droplets' size of 50 μm is assumed in these simulations. As shown in Fig. 1, polyhedral meshes are utilized in the computational model to decrease the computation time while maintaining the accuracy of the results.

The schematics of the building, wind-catcher, and the outlet window opening are shown in Supplemental Fig. S1. In addition, the dimensions and the location of the water spray are shown in this figure. The figure shows that the water is injected near the wind-catcher inlet. The guide vanes suggested by Alsailani et al. [31] are used to obtain a higher flow uniformity within the wind-catcher. In addition, the effects of an internal baffle with different angles, β, on the CFD results are also studied.

Results and discussions

It should be noted that Supplemental Fig. S2 shows the results of grid sensitivity analysis, whereas Supplemental Figs. S3 and S4 show the results of model validation. This section examines the outcomes of the model.

Effect of geometrical design of wind-catcher

In this study, the wind-catcher entrance to the room is modified for better airflow circulation. Supplemental Fig. S5 shows the new modified design of the wind-catcher and the conventional geometry, including the air velocity vector. The angle between the lower horizontal line and the vertical axis of the modified design is 45°. The velocity vector fields

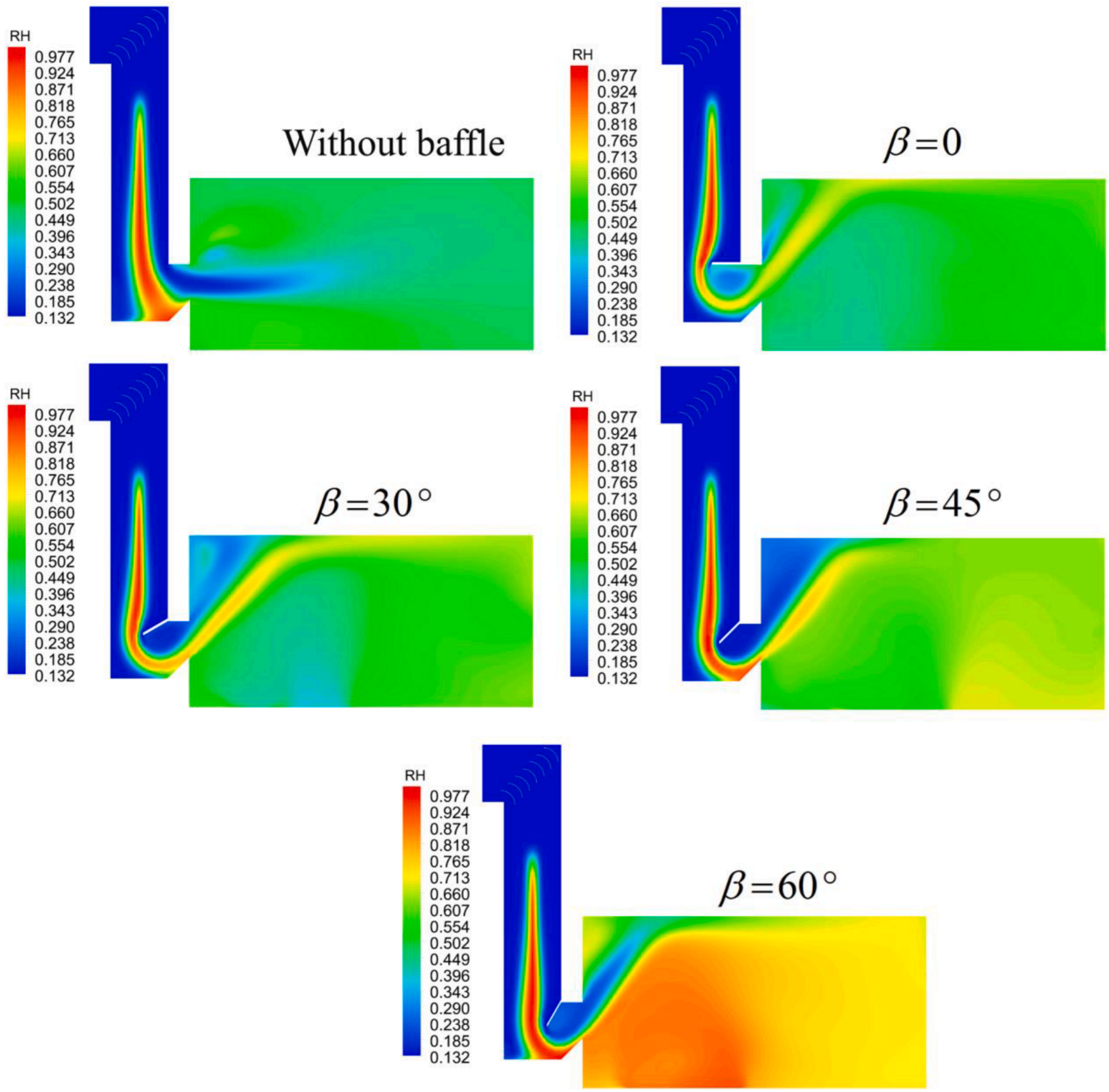

Fig. 4. The relative humidity (RH) contours on the building mid-section for different wind-catchers baffle angles.

show that the air distribution within the room for the wind-catcher with the inclined surface is more uniform than the conventional geometry and those reported in the literature for the original design [27,29,37]. This modification to the wind-catcher outlet improves room flow uniformity and provides the injected water droplets more time to evaporate, improving occupants' thermal comfort.

Supplemental Fig. S6 shows the airflow streamlines in the room integrated with the wind-catcher with the inclined bottom surface. Comparing this figure with the results for the flat surface wind-catcher outlet reported in [27,29,37] shows that the wind-catcher with the inclined surface leads to a better airflow distribution in the room. In addition, the residence time is longer compared to the flat surface outlet case.

The effect of the inclined bottom surface of the wind-catcher outlet in the room was examined in the last section. This section investigates the influence of a baffle near the wind-catcher outlet on its performance.

Fig. 2 shows air velocity contours on the building's central plane for 39.2 °C inlet air temperature and 0.004 kg/s water droplet flow rate. As reported in [31], the guide vanes installed at the top of the tower make airflow relatively uniform inside wind-catchers with different baffle angles. Fig. 2 shows noticeable differences in airflow velocity pattern in the room for the cases of wind-catchers with and without a baffle. The baffle directs the airflow toward the room ceiling. The inlet airflow pattern changes slightly as the baffle angle β increases from the horizontal axis. It is observed that wind-catchers with baffles have a more uniform velocity distribution than those without the baffle.

Fig. 2 also provides additional insights into the outdoor airflow behavior when a baffle is installed on the wind-catcher with $\beta = 60°$. A flow separation zone and the wake behind the building are visible on the roof. A noticeable stagnation area on the wind catcher's ceiling results from the direct influence of the flow on this region. The airflow is bent downwards the tower of the wind-catcher. Similar results were reported in earlier studies in the field [28]. In addition, a separate flow forms at the lower side of the window.

Fig. 3 shows the air temperature contours on the mid-plane of the building for an inlet air temperature of 39.2 °C, a water spray droplet flow rate of 0.004 kg/s, and the wind air velocity profile as given by Eqs. (1)–(3) with a free-stream velocity of 2.7 m/s. As expected, the minimum airflow temperature is observed near the water spray region. Moreover, the maximum airflow temperature is found in the wind-

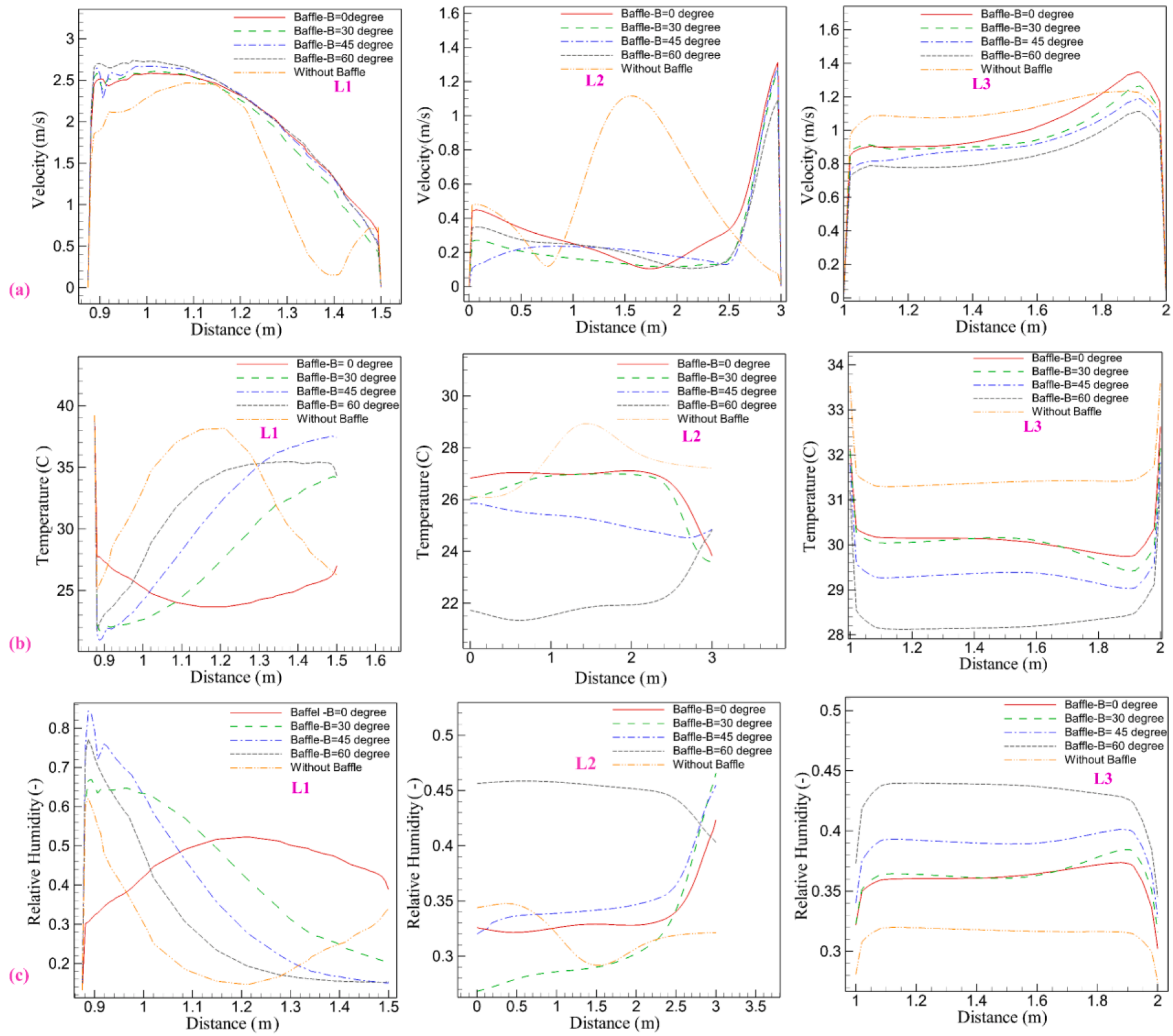

Fig. 5. Predicted air velocity profiles, (a), temperature profiles, (b), and the RH profiles, (c), at different sections in the room.

catcher tower, far away from the water droplets. There is a noticeable difference in air temperature distribution in the room for wind-catchers with or without baffles. That is, the wind-catcher baffles significantly influence the room air temperature. Although the baffles with different angles show similar behaviors, the baffle with $\beta = 30^{\circ}$ exhibits the highest temperature in the first half of the room, and the wind-catch with $\beta = 60^{\circ}$ baffle exhibits the lowest temperature in the room. These trends can be attributed to the distribution of cooled air by these baffles. Moreover, the air temperature distribution in the room with the wind-catcher with $\beta = 60^{\circ}$ baffle is more uniform than in the other cases.

Fig. 4 shows relative humidity contour plots on the building central plane for an inlet air temperature of 39.2 °C, 13.2 % humidity, 0.006 kg/s water droplet mass flow rate, and 2.7 m/s free-stream airflow velocity. It is seen that the presence and absence of wind-catchers baffle and baffle angles affect the room humidity. In particular, the baffle angle markedly affects the relative humidity distribution in the room. Interestingly, these contours show the opposite trend to the air temperature contours shown in Fig. 3, so that the room with the highest RH corresponds to that with the lowest air temperature.

Fig. 4 indicates that the maximum relative humidity occurs near the water spray where water is injected. The airflow convects the relative humidity in the tower and through the room. The baffle angles significantly affect the vapor distribution in the room. The one with $\beta = 30^{\circ}$ leads to the lowest vapor concentration, especially in the first half of the room, while the baffle with $\beta = 60^{\circ}$ has the highest vapor fraction in this section and the entire room. Also, a wind-catcher with $\beta = 60^{\circ}$ baffle predicts the highest RH values in the room, among different baffle angles. This may be because water droplets stay in the room longer.

Fig. 5 shows the local air velocity profiles, temperature profiles, and RH profiles in three vertical lines at mid-section, namely, the wind-catcher room entrance, L1, the middle of the room, L2, and the open window outlet, L3. Here the airflow temperature of 39.2 °C, a water droplet flow rate of 0.004 kg/s, and the free-stream airflow velocity of 2.7 m/s at the inlet of the computational domain are assumed.

The distribution of airflow velocity, temperature, and relative humidity along the vertical lines at the loom inlet, middle of the room, and at the window sections are shown in Fig. 5. Fig. 5a shows that the velocity profiles at the room inlet from the wind-catchers with inclined baffles are roughly the same. However, there are differences between these profiles and that for the wind-catcher without a baffle. The differences in velocity profiles in the middle of the room and the window opening for the wind-catchers with various inclined baffles become larger than the inlet section. According to the figure, the flow pattern in the middle of the room for a wind-catcher without a baffle is different from those for the wind-catchers with baffles. The baffled wind-catcher with $\beta = 60^{\circ}$ exhibits the highest air velocity at the room entrance. In contrast, the unbaffled wind-catcher leads to the highest air velocity in

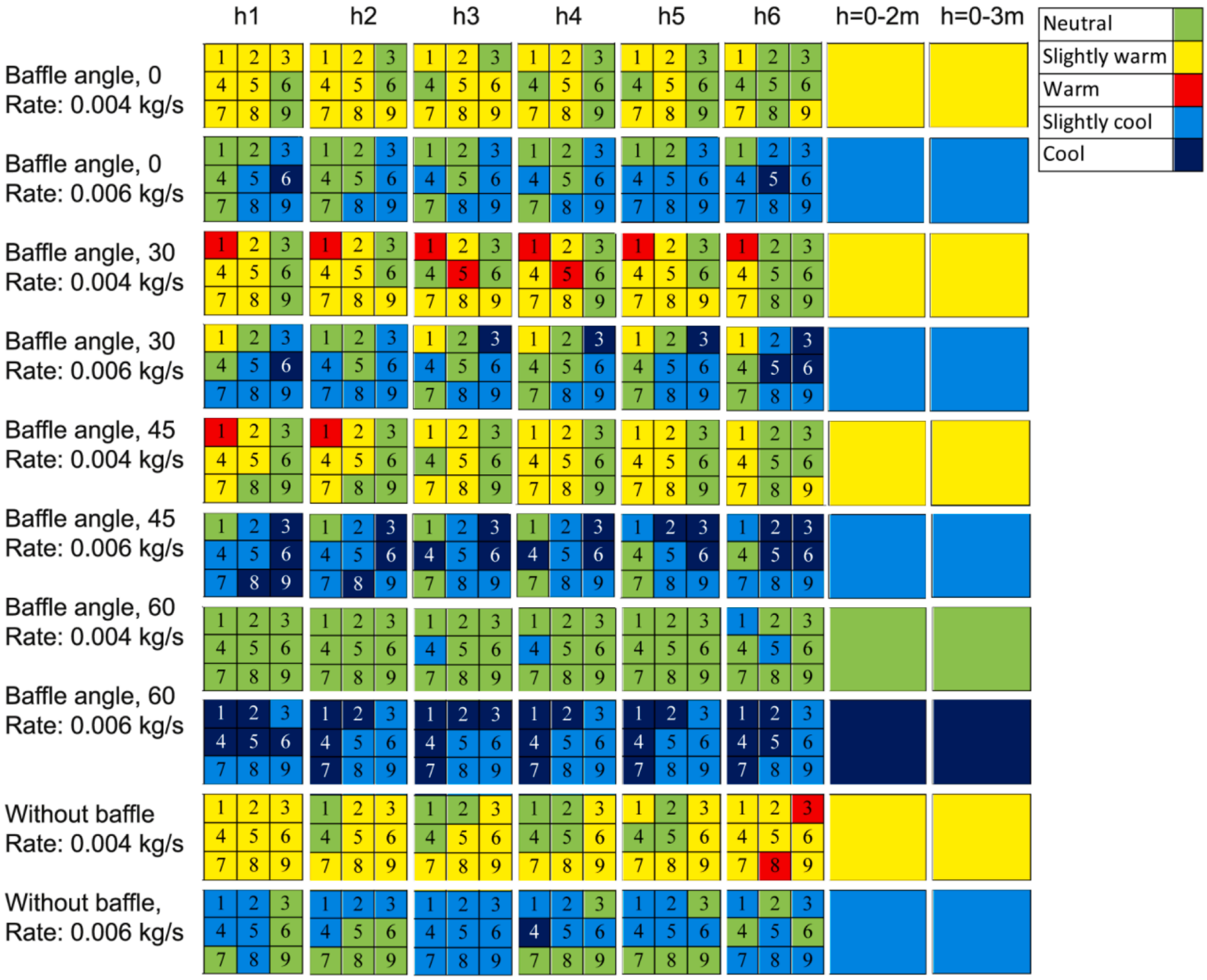

Fig. 6. Evaluation of thermal comfort at different zones for spray rates of 0.004 and 0.006 kg/s.

the middle of the room and at the window opening outlet.

Fig. 5b shows that the temperature profiles at all three sections of the room for the wind-catchers with inclined baffles differ from each other. The horizontal baffle shows a different temperature profile in the room inlet compared to other cases. However, there is a significant difference in temperature profiles in the middle of the room and the window opening for the wind-catchers with and without baffles. The differences between the temperature profiles of baffled wind-catchers are due to the evaporation of spray droplets in the wind-catcher that changes with the baffle angle. The wind-catcher without baffle exhibits the highest air temperature at all studied sections, while the wind-catcher with baffle $\beta = 60^\circ$ leads to the lowest air temperature in the sections in the middle of the building and at the window opening.

As shown in Fig. 5c, the wind-catcher with a horizontal baffle shows a different relative humidity profile at the room entrance compared to the other baffled wind-catchers. The wind-catcher without baffle exhibits the lowest relative humidity profiles for almost all studied sections. Conversely, the wind-catcher with $\beta = 60^\circ$ baffle exhibits the highest water concentration in the middle of the room and the window opening outlet.

Supplemental Fig. S7 displays the contour plots of the temperature, relative humidity, and airflow velocity on the horizontal planes at two levels of 0.75 and 2.25 m from the floor in the room with the wind-catcher with $\beta = 60^\circ$ baffle and an inlet air temperature of 39.2 °C, a water droplet flow rate of 0.004 kg/s, and the wind air velocity profile as given by Eqs. (1)–(3) with a free-stream velocity of 2.7 m/s. It is seen that the distribution of the air velocity, air temperature, and relative humidity are roughly uniform, except near the entrance region of the room.

Thermal comfort analysis

Various factors affect the comfort conditions, including the environment and individual factors [50]. The climatological and field studies are the most prevalent methods for thermal comfort analysis. Therefore, similar to the studies of [16,37], indoor thermal comfort is evaluated in the present study by considering the CFD results for temperature, velocity, and relative humidity as input conditions in the CBE thermal comfort tool. The code calculates thermal comfort according to ASHRAE 55–2020.

The room interior is divided into fifty-four regions, as shown in Supplemental Fig. S8, to evaluate the zonal thermal comfort conditions. The information is then used to assess the capability of the wind-catcher system to provide good comfort conditions for the room occupants.

The thermal comfort results for cases are presented in Fig. 6. Note that in all cases, the evaporative cooling by water spray injection is computed by the CFD model for each zone at each level and is considered part of the PMV calculation. This figure provides the thermal comfort results for the different zones, for the outdoor airflow velocity of 3.7 m/s, the temperature of 39.2 °C, and two water spray rates of 0.004 and 0.006 kg/s.

The thermal comfort values are also calculated in levels of 0 to 2 m in the room and 0 to 3 m (entire room) in addition to the zones shown in Supplemental Fig. S8. Fig. 6 shows that the wind-catcher with baffle $\beta =$

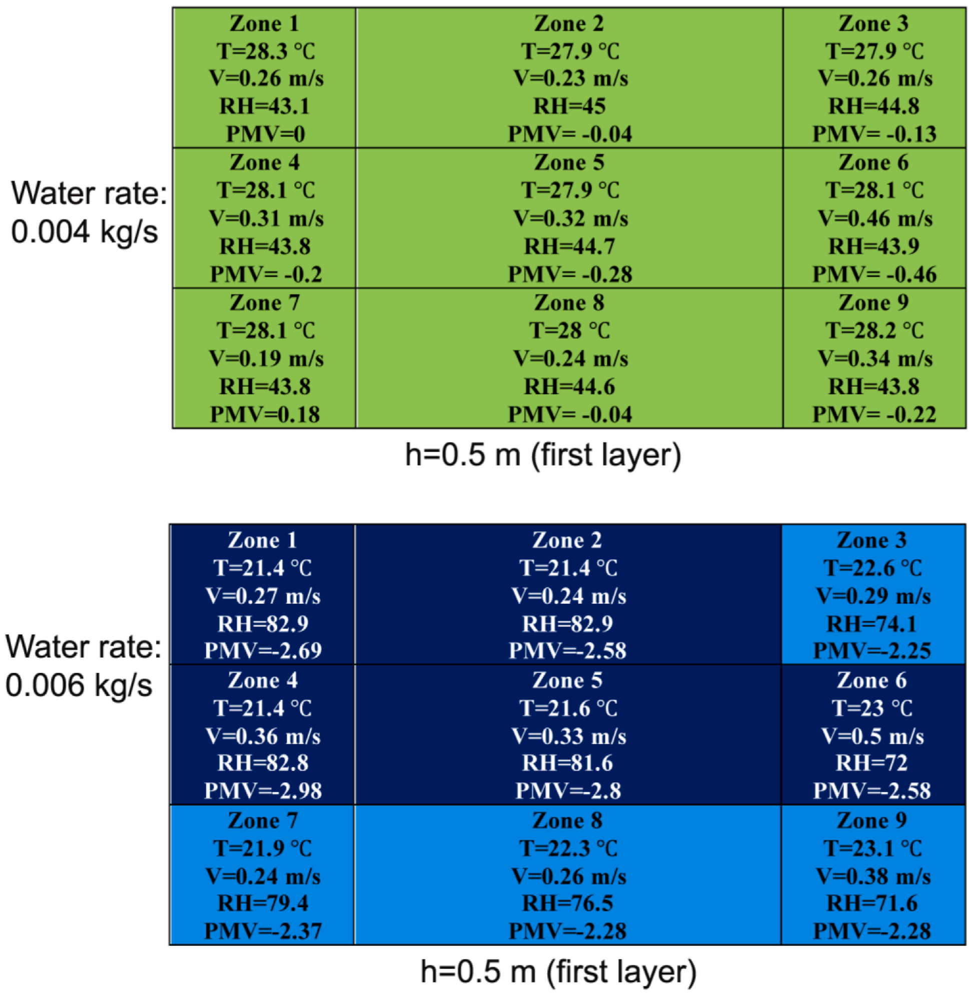

Fig. 7. Defined thermal comfort of nine zones at the first layer near the floor for the wind-catcher with baffle $\beta = 60^\circ$ for various water spray flow rates.

60° provides the best indoor thermal comfort conditions for the occupants at all levels for the water rate of 0.004 kg/s based on the simulated conditions. This case also provides the neutral status for both $0-2$ m and $0-3$ m levels. Even so, the wind-catcher with baffle $\beta = 60^\circ$ provides a slightly-cool and cool condition in different room' zones at every level. This case also exhibits the cool conditions for both levels of $0-2$ m and $0-3$ m. That is, the thermal comfort is affected not only by the design of the wind-catcher but also by the rate of spray water injection. According to Fig. 6, the baffled wind-catchers with$\beta = 0$, 30, 45, and 60° and unbaffled wind-catcher all lead to the slightly-cool and cool conditions for the 0.006 kg/s spray water flow rate. Therefore, the mass flow of injected water has a dominant effect on thermal comfort.

Fig. 7 presents the mean velocity, temperature, and relative humidity for the nine zones at the first layer near the floor (Supplemental Fig. S8) for the case of the wind-catcher with the baffle angle of $\beta = 60^\circ$ and water spray flow rates of 0.004 and 0.006 kg/s. Fig. 7 indicates that a higher water flow rate results in higher relative humidity in the room, decreasing the mean air temperature at different zones in the first layer ($h = 0.5$ m). Furthermore, since the water droplets are moving in the same direction as the airflow, the momentum exchanges are more prominent in the tower and the room, so with increasing the water flow rate, the flow velocity increases in the different zones. Also, it can be seen that the relative humidity increases with the spray water flow rate.

Conclusions

This study used the Eulerian-Lagrangian multiphase technique to simulate direct-air evaporative cooling in a one-sided wind-catcher integrated with a typical size room. The developed computational model could accurately predict the airflow behavior in the tower and the room. Furthermore, the current model simulated the evaporative cooling by spray water injection with reasonable accuracy. Finally, a one-side wind-catcher design was studied to improve the resident's thermal comfort and air ventilation.

It was shown that the new wind-catcher design, with an inclining the bottom surface and with a baffle, resulted in a uniform distribution of airflow velocity, air temperature, relative humidity, and longer residence time of droplets inside the building. The baffle angle, β, was identified as a controlling factor for the building's airflow speed and direction. Furthermore, it was found that the humidity distribution in the building due to the evaporative cooling is inversely proportional to the airflow temperature. That is, an increase in relative humidity is directly correlated with a decrease in the room's air temperature. The wind-catcher with a baffle angle of $\beta = 60^\circ$ provided the lowest temperature and the highest RH in the room, particularly in the middle of the room (L2 region) and the open window outlet L3 region).

Thermal comfort was evaluated using the CFD results for temperature, velocity, and relative humidity as input conditions into the CBE thermal comfort tool. The room interior was divided into fifty-four regions, and the thermal comfort in various zones was evaluated. It was found that the thermal comfort was affected not only by the wind-catcher's design but also by the spray water injection rate. For the spray water rate of 0.004 kg/s, the best indoor comfort conditions for the occupants were obtained by the wind-catcher with $\beta = 60^\circ$ baffle at all building levels. Furthermore, it was observed that the spray water flow rate of 0.004 kg/s was sufficient to provide good comfort levels in the building when the outdoor air was at 39.2 °C, and the wind speed was 2.7 m/s. Overall, the wind-catcher/spray system reduced the air temperature inside the building up to 17.4 °C.

Based on the presented results, it was clear that the evaporative cooling system must include a control strategy with sensors to provide optimum comfort levels. For example, the spray water injection must be reduced to the optimum level when the outdoor air humidity increases. In addition, other variables, such as outdoor temperature and wind velocity, must be considered in optimizing thermal comfort. Studies of the influence of surrounding building clusters with a range of heights in an urban setting on the inlet air velocity and the wind-catcher system efficiency are left for future studies.

CRediT authorship contribution statement

Jamal Foroozesh: Software, Methodology. **S.H. Hosseini:** Writing – original draft, Conceptualization, Methodology, Investigation. **A.J. Ahmadian Hosseini:** Investigation, Writing – review & editing. **F. Parvaz:** Investigation, Supervision. **K. Elsayed:** Investigation, Supervision. **Nihan Uygur Babaoğlu:** Investigation, Supervision. **K. Hooman:** Investigation, Writing – review & editing. **G. Ahmadi:** Conceptualization, Writing – review & editing.

Declaration of Competing Interest

The authors declare that they have no known competing financial interests or personal relationships that could have appeared to influence the work reported in this paper.

Data availability

Data will be made available on request.

Appendix A. Supplementary data

Supplementary data to this article can be found online at https://doi.org/10.1016/j.seta.2022.102736.

References

[1] UK Government Climate Change Act 2008 (c27) The Stationery Office Ltd, London (2008). n.d.
[2] Calautit JK, Hughes BR, Nasir DS. Climatic analysis of a passive cooling technology for the built environment in hot countries. Appl Energy 2017;186:321–35. https://doi.org/10.1016/j.apenergy.2016.05.096.
[3] Nejat P, Calautit JK, Majid MZA, Hughes BR, Zeynali I, Jomehzadeh F. Evaluation of a two-sided windcatcher integrated with wing wall (as a new design) and comparison with a conventional windcatcher. Energy Build 2016;126:287–300. https://doi.org/10.1016/j.enbuild.2016.05.025.
[4] Calautit JK, Chaudhry HN, Hughes BR, Ghani SA. Comparison between evaporative cooling and a heat pipe assisted thermal loop for a commercial wind tower in hot and dry climatic conditions. Appl Energy 2013;101:740–55. https://doi.org/10.1016/j.apenergy.2012.07.034.
[5] Elaouzy Y, el Fadar A. A multi-level evaluation of bioclimatic design in Mediterranean climates. Sustain Energy Technol Assess 2022;52:102124. https://doi.org/10.1016/j.seta.2022.102124.
[6] William MA, Suárez-López MJ, Soutullo S, Hanafy AA. Building envelopes toward energy-efficient buildings: A balanced multi-approach decision making. Int J Energy Res 2021;45:21096–113. https://doi.org/10.1002/er.7166.
[7] Nasruddin S, Satrio P, Mahlia TMI, Giannetti N, Saito K. Optimization of HVAC system energy consumption in a building using artificial neural network and multi-objective genetic algorithm. Sustain Energy Technol Assess 2019;35:48–57. https://doi.org/10.1016/j.seta.2019.06.002.
[8] Yao R, Zhang S, Du C, Schweiker M, Hodder S, Olesen BW, et al. Evolution and performance analysis of adaptive thermal comfort models – A comprehensive literature review. Build Environ 2022;217:109020. https://doi.org/10.1016/J.BUILDENV.2022.109020.
[9] Taleb HM. Natural ventilation as energy efficient solution for achieving low-energy houses in Dubai. Energy Build 2015;99:284–91. https://doi.org/10.1016/j.enbuild.2015.04.019.
[10] Khalili M, Amindeldar S. Traditional solutions in low energy buildings of hot-arid regions of Iran. Sustain Cities Soc 2014;13:171–81. https://doi.org/10.1016/j.scs.2014.05.008.
[11] Cuce E, Sher F, Sadiq H, Cuce PM, Guclu T, Besir AB. Sustainable ventilation strategies in buildings: CFD research. Sustainable Energy Technol Assess 2019;36. https://doi.org/10.1016/j.seta.2019.100540.
[12] Calautit JK, Hughes BR. Wind tunnel and CFD study of the natural ventilation performance ofa commercial multi-directional wind tower. Build Environ 2014;80:71–83. https://doi.org/10.1016/j.buildenv.2014.05.022.
[13] Saadatian O, Sopian K, Lim CH, Asim N, Sulaiman MY. Trombe walls: A review of opportunities and challenges in research and development. Renew Sustain Energy Rev 2012;16:6340–51. https://doi.org/10.1016/j.rser.2012.06.032.
[14] Montazeri H. Experimental and numerical study on natural ventilation performance of various multi-opening wind catchers. Build Environ 2011;46:370–8. https://doi.org/10.1016/j.buildenv.2010.07.031.
[15] Bahadori MN. Passive cooling systems in Iranian architecture. Renewable Energy: Four Volume Set 2018;1–4:87–101. https://doi.org/10.4324/9781315793245-10.
[16] Hosseini SH, Shokry E, Ahmadian Hosseini AJ, Ahmadi G, Calautit JK. Evaluation of airflow and thermal comfort in buildings ventilated with wind catchers: Simulation of conditions in Yazd City. Iran Energy Sustain Dev 2016;35:7–24. https://doi.org/10.1016/j.esd.2016.09.005.
[17] Mostafaeipour A, Bardel B, Mohammadi K, Sedaghat A, Dinpashoh Y. Economic evaluation for cooling and ventilation of medicine storage warehouses utilizing wind catchers. Renew Sustain Energy Rev 2014;38:12–9. https://doi.org/10.1016/j.rser.2014.05.087.
[18] Chenari B, Dias Carrilho J, Gameiro Da Silva M. Towards sustainable, energy-efficient and healthy ventilation strategies in buildings: A review. Renew Sustain Energy Rev 2016;59:1426–47. https://doi.org/10.1016/j.rser.2016.01.074.
[19] O'Connor D, Calautit JK, Hughes BR. A study of passive ventilation integrated with heat recovery. Energy Build 2014;82:799–811. https://doi.org/10.1016/j.enbuild.2014.05.050.
[20] Khan N, Su Y, Riffat SB. A review on wind driven ventilation techniques. Energy Build 2008;40:1586–604. https://doi.org/10.1016/j.enbuild.2008.02.015.
[21] Calautit JK, O'Connor D, Hughes BR. Determining the optimum spacing and arrangement for commercial wind towers for ventilation performance. Build Environ 2014;82:274–87. https://doi.org/10.1016/j.buildenv.2014.08.024.
[22] Saffari H, Hosseinnia SM. Two-phase Euler-Lagrange CFD simulation of evaporative cooling in a Wind Tower. Energy Build 2009;41:991–1000. https://doi.org/10.1016/j.enbuild.2009.05.006.
[23] Jomehzadeh F, Nejat P, Calautit JK, Yusof MBM, Zaki SA, Hughes BR, et al. A review on windcatcher for passive cooling and natural ventilation in buildings, Part 1: Indoor air quality and thermal comfort assessment. Renew Sustain Energy Rev 2017;70:736–56. https://doi.org/10.1016/j.rser.2016.11.254.
[24] Sadeghi H, Kalantar V. Performance analysis of a wind tower in combination with an underground channel. Sustain Cities Soc 2018;37:427–37. https://doi.org/10.1016/j.scs.2017.12.002.
[25] Badran AA. Performance of cool towers under various climates in Jordan. Energy Build 2003;35:1031–5. https://doi.org/10.1016/S0378-7788(03)00067-7.
[26] Hughes BR, Calautit JK, Ghani SA. The development of commercial wind towers for natural ventilation: A review. Appl Energy 2012;92:606–27. https://doi.org/10.1016/j.apenergy.2011.11.066.
[27] Goudarzi N, Sheikhshahrokhdehkordi M, Khalesi J, Hosseiniirani S. Airflow and thermal comfort evaluation of a room with different outlet opening sizes and elevations ventilated by a two-sided wind catcher. J Build Eng 2021;37:102112. https://doi.org/10.1016/j.jobe.2020.102112.
[28] Montazeri H, Montazeri F. CFD simulation of cross-ventilation in buildings using rooftop wind-catchers: Impact of outlet openings. Renew Energy 2018;118:502–20. https://doi.org/10.1016/j.renene.2017.11.032.
[29] Reyes VA, Sierra-Espinosa FZ, Moya SL, Carrillo F. Flow field obtained by PIV technique for a scaled building-wind tower model in a wind tunnel. Energy Build 2015;107:424–33. https://doi.org/10.1016/j.enbuild.2015.08.047.
[30] Varela-Boydo CA, Moya SL. Inlet extensions for wind towers to improve natural ventilation in buildings. Sustain Cities Soc 2020;53:101933. https://doi.org/10.1016/j.scs.2019.101933.
[31] Alsailani M, Montazeri H, Rezaeiha A. Towards optimal aerodynamic design of wind catchers: Impact of geometrical characteristics. Renew Energy 2021;168:1344–63. https://doi.org/10.1016/j.renene.2020.12.053.
[32] Kalantar V. Numerical simulation of cooling performance of wind tower (Baud-Geer) in hot and arid region. Renew Energy 2009;34:246–54. https://doi.org/10.1016/j.renene.2008.03.007.
[33] Ahmadikia H, Moradi A, Hojjati M. Performance analysis of a wind-catcher with water spray. Int J Green Energy 2012;9:160–73. https://doi.org/10.1080/15435075.2011.622019.
[34] Montazeri H, Montazeri F, Azizian R, Mostafavi S. Two-sided wind catcher performance evaluation using experimental, numerical and analytical modeling. Renew Energy 2010;35:1424–35. https://doi.org/10.1016/j.renene.2009.12.003.
[35] Sadeghi M, de Dear R, Samali B, Wood G. Optimization of wind tower cooling performance: A wind tunnel study of indoor air movement and thermal comfort. Procedia Eng 2017;180:611–20. https://doi.org/10.1016/j.proeng.2017.04.220.
[36] Bouchahm Y, Bourbia F, Belhamri A. Performance analysis and improvement of the use of wind tower in hot dry climate. Renew Energy 2011;36:898–906. https://doi.org/10.1016/j.renene.2010.08.030.
[37] Reyes VA, Moya SL, Morales JM, Sierra-Espinosa FZ. A study of air flow and heat transfer in building-wind tower passive cooling systems applied to arid and semi-arid regions of Mexico. Energy Build 2013;66:211–21. https://doi.org/10.1016/j.enbuild.2013.07.032.

[38] Bahadori MN, Mazidi M, Dehghani AR. Experimental investigation of new designs of wind towers. Renew Energy 2008;33:2273–81. https://doi.org/10.1016/j.renene.2007.12.018.
[39] Jafari S, Kalantar V. Numerical simulation of natural ventilation with passive cooling by diagonal solar chimneys and windcatcher and water spray system in a hot and dry climate. Energy Build 2022;256:111714. https://doi.org/10.1016/j.enbuild.2021.111714.
[40] Rabani M. Performance analysis of a passive cooling system equipped with a new designed solar chimney and a water spraying system in an underground channel. Sustainable Energy Technol Assess 2019;35:204–19. https://doi.org/10.1016/j.seta.2019.07.005.
[41] ASHRAE, Standard 55-2020. Thermal environmental conditions for human occupancy. n.d.
[42] Hoyt T, Schiavon S, Piccioli A, Moon D, Steinfeld K. CBE thermal comfort tool. Center for the Built Environment, University of California Berkeley; 2013. p. 40.
[43] Sheikhshahrokhdehkordi M, Khalesi J, Goudarzi N. High-performance building: Sensitivity analysis for simulating different combinations of components of a two-sided windcatcher. J Build Eng 2020;28:101079. https://doi.org/10.1016/j.jobe.2019.101079.
[44] Nejat P, Salim Ferwati M, Calautit J, Ghahramani A, Sheikhshahrokhdehkordi M. Passive cooling and natural ventilation by the windcatcher (Badgir): An experimental and simulation study of indoor air quality, thermal comfort and passive cooling power. J Build Eng 2021;41:102436. https://doi.org/10.1016/j.jobe.2021.102436.
[45] Xu F, Xu S, Passe U, Ganapathysubramanian B. Computational study of natural ventilation in a sustainable building with complex geometry. Sustainable Energy Technol Assess 2021;45:101153. https://doi.org/10.1016/j.seta.2021.101153.
[46] Montazeri H, Blocken B, Hensen JLM. Evaporative cooling by water spray systems: CFD simulation, experimental validation and sensitivity analysis. Build Environ 2015;83:129–41. https://doi.org/10.1016/j.buildenv.2014.03.022.
[47] Franke J, Hellsten A, Schlünzen KH, Carissimo B. The COST 732 Best practice guideline for CFD simulation of flows in the urban environment: A summary. Int J Environ Pollut 2011;44:419–27. https://doi.org/10.1504/IJEP.2011.038443.
[48] Southpointe A. ANSYS Fluent User's Guide 15.0. Canonsberg, PA: ANSYS Inc; 2013.
[49] Rabani M, Kalantar V, Dehghan AA, Faghih AK. Empirical investigation of the cooling performance of a new designed Trombe wall in combination with solar chimney and water spraying system. Energy Build 2015;102:45–57. https://doi.org/10.1016/j.enbuild.2015.05.010.
[50] Givoni B. Comfort, climate analysis and building design guidelines. Energy Build 1992;18:11–23. https://doi.org/10.1016/0378-7788(92)90047-K.